JOURNAL OF MATERIALS SCIENCE 33 (1998) 1253–1262

A novel precursor for the sol–gel and CVD methods to prepare alumina permselective membranes

JU H. KIM, GUANG J. CHOI*, JOONG K. LEE, SANG J. SIM, YOUNG D. KIM, YOUNG S. CHO
Division of Chemical Engineering, Korea Institute of Science and Technology (KIST), P. O. Box 131, Cheongryang, Seoul 130-650, Korea

A novel metalorganic compound, $Al(OPr^i)_2(etac)$, was synthesized and used for the preparation of alumina permselective membranes. Membranes were produced by forming permselective thin layers on porous alumina support tubes, either by dip-coating of alumina sol, by the chemical vapour deposition (CVD) technique, or by a combination of the two. In CVD processing, a commercial precursor, $Al(OPr^i)_3$ was also studied and compared with our novel precursor. Characterization of alumina-producing materials was performed by scanning electron microscopy, X-ray diffraction, transmission electron microscopy, Fourier transform–infrared spectroscopy, thermogravimetric analysis/differential thermal analysis and ^1H-nuclear magnetic resonance. The gas separation performance of alumina permselective membranes was measured by permeation experiment using hydrogen and nitrogen gases. For each membrane, gas permeation rates and H_2/N_2 selectivity were determined. There was a significant difference in the mechanism of CVD deposition between the two compounds. The maximum H_2/N_2 selectivity among our results was attained by combining sol dip-coating techniques with CVD of our novel precursor, $Al(OPr^i)_2(etac)$.
© *1998 Chapman & Hall*

1. Introduction

Membranes to separate mixtures of gas-phase or liquid-phase in a desired purity have found a number of important industrial applications. In the past few years, the development of inorganic membranes, which particularly have the importance of certain advantages, paved the way for the application of membrane in high-temperature reactors [1–3]. Compared to polymeric membranes, ceramic membranes have an extremely high-temperature capability, which makes them suitable for metal-melting operations or applications which were required for steam cleaning. Their chemical resistance makes them virtually immune to a wide variety of solvents, acids, alkalines, and detergents. Although these performance characteristics are highly attractive to many processing industries, the ceramic membrane still has minor disadvantages, such as, its relatively high cost, the difficulty of controlling pore-size distribution, and its relative ease of crack formation. For these reasons, it has not yet been practical for commercial use.

Recently, a number of papers have been published concerning the preparation and characterization of microporous γ-alumina membranes [4–10]. The formation of membranes on the support with pores of 120 nm diameter, has been described [4]. The formation of membranes on multilayer supports with large pores has also been reported [5]. Liquid permeation and separation characteristics were measured [6–8], and, for example, a cut-off value of molecular weight of 2000 for polyethylene glycol was achieved. More recently, gas permeation characteristics of pure gases have been determined [9, 10].

In general, for the manufacture of microporous γ-alumina membranes, the sol–gel and chemical vapour deposition (CVD) methods have been used. The CVD method is one of the most widely used techniques for thin films; owing to its excellent process controllability, high uniformity, and high throughput, it has a good reproducibility in the membrane manufacturing process [11].

The sol–gel method has several advantages, such as low reaction temperature, and it is a relatively simple process. However, there is a limitation in decreasing the particle size of the sol which determines the pore size of the membranes. The sol–gel method can be manufactured in two ways [12]. First, after being hydrolysed with a precursor, such as metal alkoxide, particles are dispersed by adding acid in an aqueous system, resulting in a particulate sol with dense oxide particles whose sizes are normally greater than 10 nm. When the precursor was partially hydrolysed with a small amount of water in non-aqueous solutions, a polymeric sol was produced which has macromolecules of size less than 10 nm. Therefore, it seems

*Author to whom all correspondence should be addressed.

to be more suitable for manufacturing a ceramic membrane with a small pore size.

The precursor needed in making polymeric sol, must undergo a chemical modification in order to control the reaction rate [13, 14]. It is known that the compound with a chelating ligand is the best compound to control the reaction rate. Therefore, this was synthesized and used as a precursor.

2. Experimental procedure

2.1. Preparation of precursor and sol

A novel precursor, $Al(OPr^i)_2(etac)$, was synthesized and studied for use in the sol–gel and CVD methods, where "etac" stands for ethyl acetoacetate. The precursor was synthesized by substituting one $-OPr^i$ functionality in commercial $Al(OPr^i)_3$ (Merck Schuchard Co.) with a chelating ligand (etac), which constitutes a β-diketonate group. Benzene was used as solvent for the synthesis reaction. The reaction was conducted in a 250 ml round-bottom flask under a reflux condition (at 80 °C) for 3 h. The solvent was removed after the reaction by distillation at atmospheric pressure. The product was purified by distillation under vacuum (5 torr at 182 °C; 1 torr = 133.322 Pa). Finally, $Al(OPr^i)_2(etac)$ was obtained in a yellow liquid form. The yield, as measured, was 92%. $Al(OPr^i)_2(etac)$ was used not only as metalorganic precursor in the CVD process, but also as precursor of a polymeric sol for the dip-coating process.

The polymeric sol was prepared through a procedure found in the literature. $Al(OPr^i)_2(etac)$ (1 mol basis) was dissolved with *i*-propanol (22.0 mol) in a 250 ml three-neck flask and the solution was heated to 80 °C with vigorous agitation. Then, nitric acid (0.3 mol), diluted in *i*-propanol, was added slowly into the reactant solution. The acid content, described above, was fixed after observing that precipitates were formed during the reaction when it was either 0.2 or 0.4 mol. $Al(OPr^i)_2(etac)$ was partially hydrolysed to produce polymeric sol with the addition of small amount of deionized water (1.0 mol). A higher water content caused premature gelation in sol solutions during the hydrolysis. The reaction time was 5 h; it was found that a reaction time longer than 5 h substantially reduced the shelf life of the sol solution prior to use, whereas a shorter reaction time frequently resulted in a poor dip-coating.

2.2. Membrane preparation by the sol–gel method

Porous alumina support tubes were purchased from Dongseo Inc., Seoul, Korea. According to the manufacturer's data, those tubes are made of α-alumina with a porosity of 34%. The average diameter of pores was known to be 0.1 μm. Tubes were cut into 8 cm long sections using a diamond cutter. The outside diameter was 10 mm while the thickness was 1.5 mm.

The dip-coating of alumina tubes in sol solutions was performed using the apparatus shown in Fig. 1. The pressure in the dip-coating chamber was varied from 100–800 kPa using a gas pressure regulator

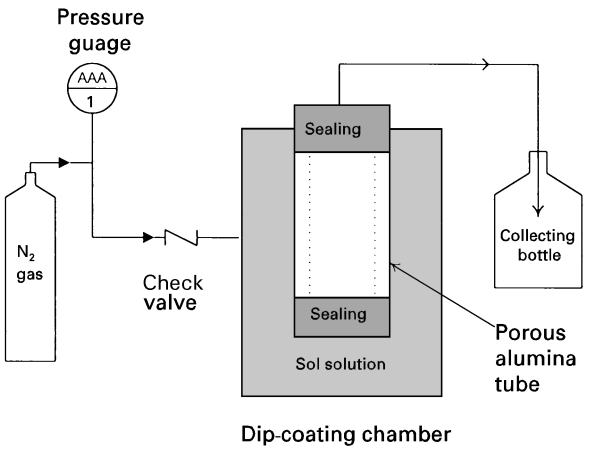

Figure 1 Apparatus for dip-coating of alumina support tubes at various pressures.

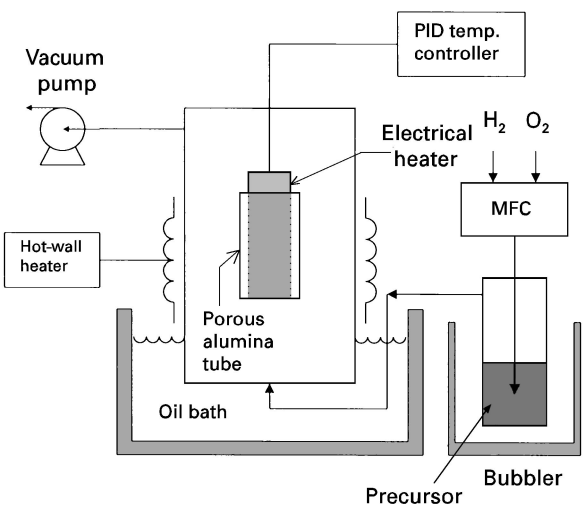

Figure 2 Schematic diagram of the hot-wall MOCVD system.

(Matheson). The dip-coating was performed by varying the dipping time from 10–60 min at an optimal pressure. Dip-coated tubes were dried at room temperature for 24 h in air, followed by the drying in a vacuum oven for 24 h. Dried tubes were calcined in a tube furnace under an oxygen atmosphere at the peak temperature of 600 °C. The heating rate was $1\ ^\circ C\ min^{-1}$. For some tubes, the effect of multiple dip-coating was investigated by varying the number of coatings from one to five. The subsequent dip-coating was carried out on calcined tubes.

2.3. Membrane preparation by the CVD method

Two precursors were used in the CVD study: $Al(OPr^i)_3$ (as-purchased) and $Al(OPr^i)_2(etac)$ (as-synthesized-and-purified). Fig. 2 shows a schematic diagram of our hot-wall MOCVD system. The vapour of each precursor was produced using a bubbler. The feeding rate of precursors was varied by adjusting the bubbler temperature: 135 °C for $Al(OPr^i)_3$ and 30 °C for $Al(OPr^i)_2(etac)$. Mixtures of oxygen and nitrogen in various compositions were used as carrier gas. The reactor wall temperature was kept constant for each precursor at 135 and 100 °C, respectively, using an electrical heating tape. The deposition temperatures

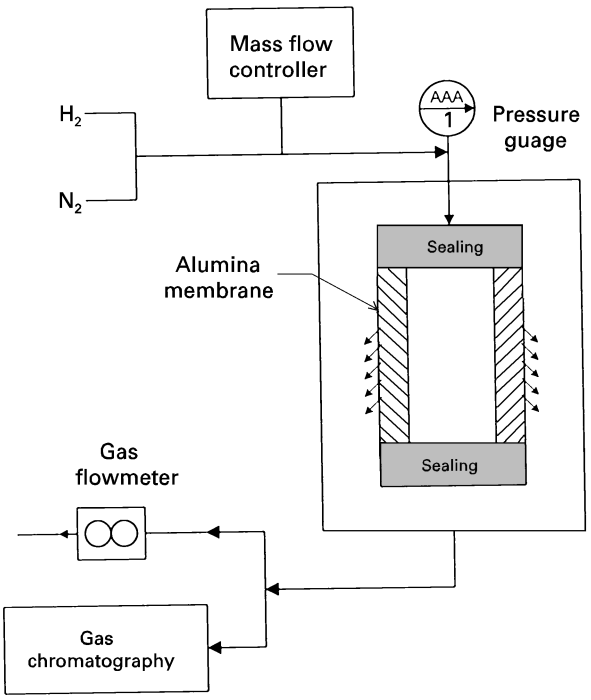

Figure 3 Apparatus for the gas permeation experiment.

were varied from 340–400 °C for $Al(OPr^i)_3$ and from, 360–460 °C for $Al(OPr^i)_2$(etac) precursors. The deposition times were 1 min for $Al(OPr^i)_3$ and 30 min for $Al(OPr^i)_2$(etac). Alumina membrane tubes which underwent CVD were calcined at 600 °C, as described above.

For some tubes, dip-coating and CVD were combined to fabricate a permselective alumina layer. CVD followed the calcination of dip-coated alumina tubes. In this case, dip-coating was performed at 400 kPa for a single layer for 20 min. CVD was carried out at 360 °C using $Al(OPr^i)_3$ as precursor. All specimens were finally calcined at 600 °C, prior to characterization.

2.4. Membrane characterization

Alumina tubes, prepared by either the sol–gel or the CVD method, were characterized via infrared spectroscopy (IR; Nicolet Magna 750), ^{1}H-nuclear magnetic resonance spectrometer (NMR; Varian Gemini300), field-emission scanning electron microscopy (FE–SEM; Hitachi S-4200), X-ray diffractometry (XRD; Rigaku S/MAX-E) with a CuK_α source, transmission electron microscopy (TEM; Philips CM30), and gas permeation measurements. Scanning electron micrographs were acquired for surfaces and cross-sections of permselective alumina layers. Fig. 3 illustrates the schematic diagram of gas permeation experiment. The gases used in the permeation experiments were hydrogen and nitrogen. Each gas, at $\Delta P = 1.0$ atm, permeated through a permselective alumina membrane tube prior to the gas flow-rate measurement using a gas flowmeter (ADM-100).

3. Results and Discussion

3.1. Precursor and sol

Fig. 4 shows the ^{1}H-NMR spectrum of $Al(OPr^i)_2$(etac). It was confirmed that diketonate substitutes one *i*-propoxyl group in $Al(OPr^i)_3$ to give rise to peaks near 5.2, 4.3, and 1.2 p.p.m. The IR spectrum of as-synthesized-and-purified $Al(OPr^i)_2$(etac) is presented in Fig. 4a. In contrast to that of $Al(OPr^i)_3$, there are two peaks near 1450 and 1600 cm^{-1}. Both peaks correspond to the existence of carbonyl groups which originate from the "etac" ligand.

The reaction for sol formation was confirmed via IR analysis. The peak for the hydroxyl group at 3400–3500 cm^{-1}, which was detected fairly weakly in the IR spectrum (Fig. 5a) of precursor $Al(OPr^i)_2$(etac), became large in that of the sol (Fig. 5b). According to a light scattering analysis, the average diameter of polymeric sol molecules was measured as 2–4 nm depending upon the reaction conditions. The typical average size of particulate alumina sol molecules is known to be greater than 10 nm. Our polymeric sols, due to their size factor, are believed to give membranes of a nanostructure more suitable for improved gas-separation performance.

Fig. 6 presents the TGA/DTA analysis results of dried sol. The weight abruptly decreases in the

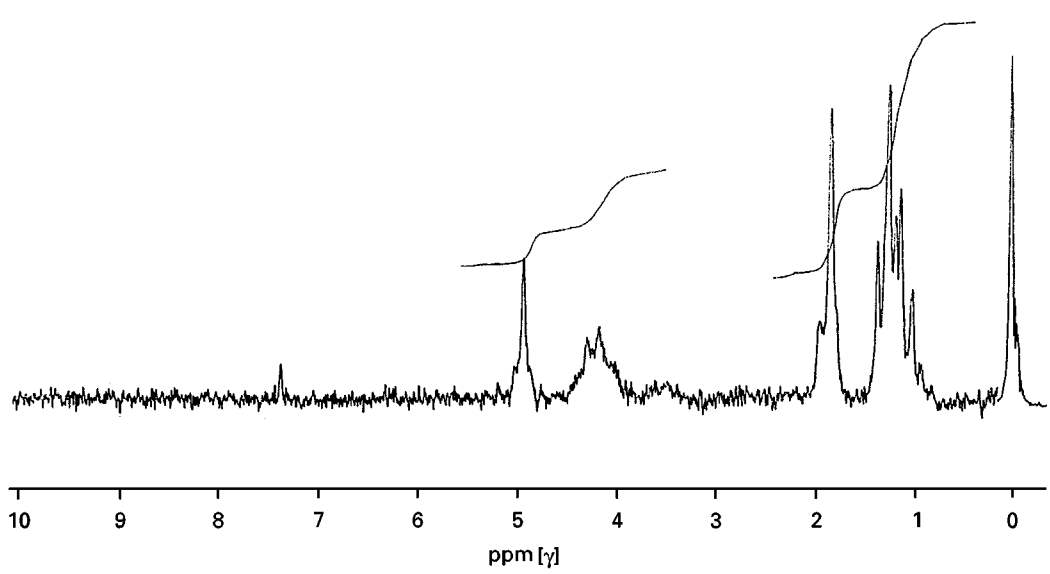

Figure 4 ^{1}H-NMR spectrum of $Al(OPr^i)_2$(etac).

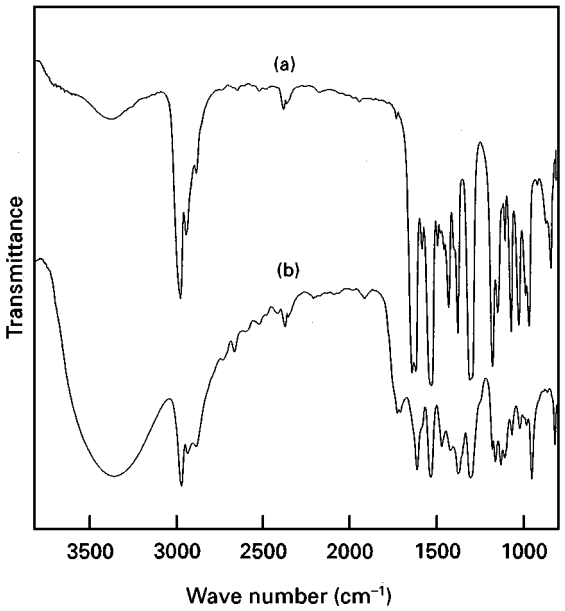

Figure 5 FT–IR spectra of (a) $Al(OPr^i)_2(etac)$ and (b) its sol.

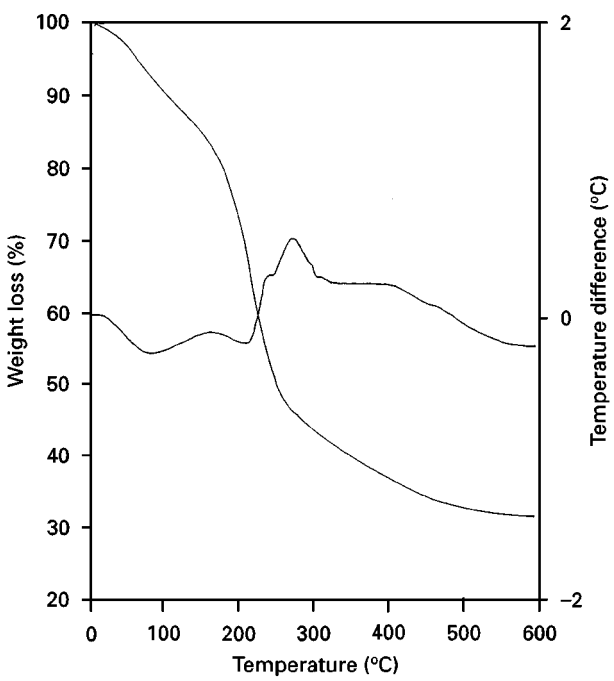

Figure 6 TGA/DTA spectra of dried sol derived from $Al(OPr^i)_2(etac)$.

120–200 °C region, probably due to the elimination of hydrated water molecules. At 200–500 °C, the weight steadily decreases as the temperature rises. In the 550–900 °C region, no appreciable weight change was observed. The IR spectrum of the sol calcined at 600 °C, does not have any peaks which could be related to organic or hydroxyl groups. Fig. 7 shows a typical XRD pattern of alumina sols after a calcination at 600 °C. The three largest peaks are correlated to (3 1 1), (4 0 0) and (4 4 0) orientations of γ-alumina crystallites. No peaks for α-alumina phase were observed. Hence, all membranes prepared by the sol–gel dip-coating technique were calcined at 600 °C throughout this study.

Fig. 8 shows (a) a bright-field image and (b) an electron diffraction pattern of sol particles after

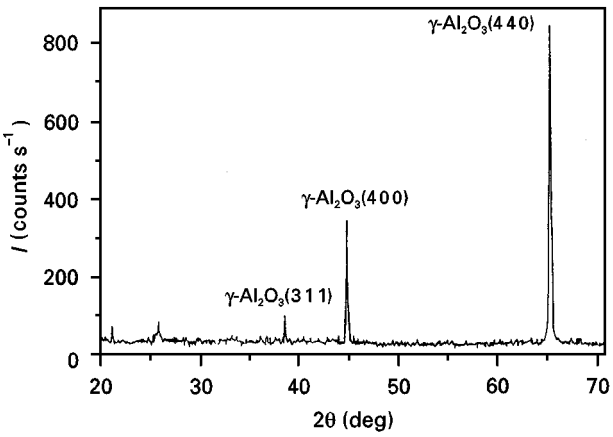

Figure 7 XRD pattern of alumina sol calcined at 600 °C.

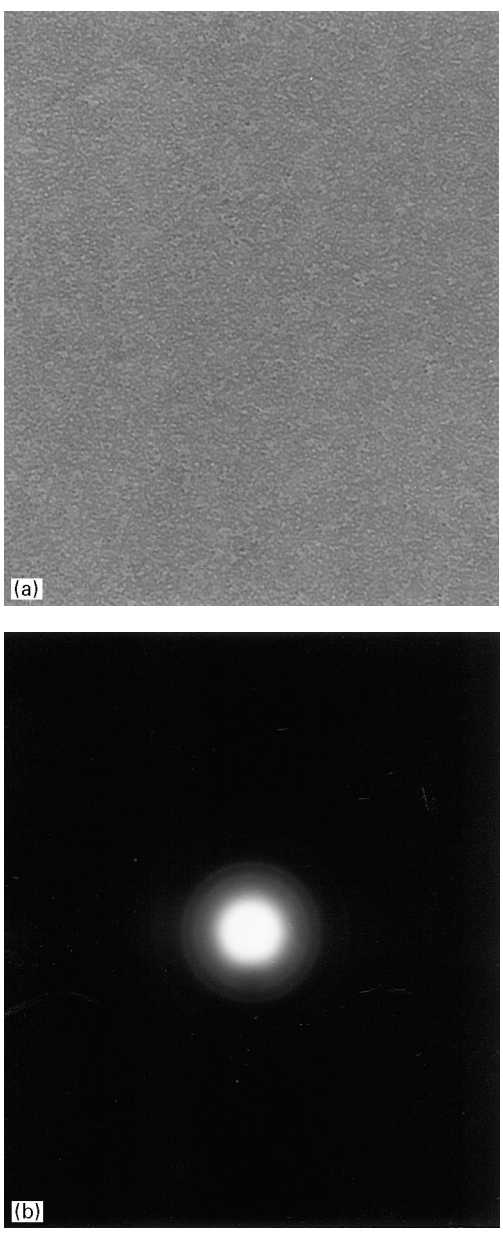

Figure 8 Transmission electron micrographs: (a) bright-field image and (b) diffraction pattern of the calcined sol.

calcination at 600 °C. Fig. 8a indicates that calcined alumina particles are composed of extremely tiny crystallites whose grain sizes look much smaller than 50 nm. Fig. 8b shows many diffuse rings around the

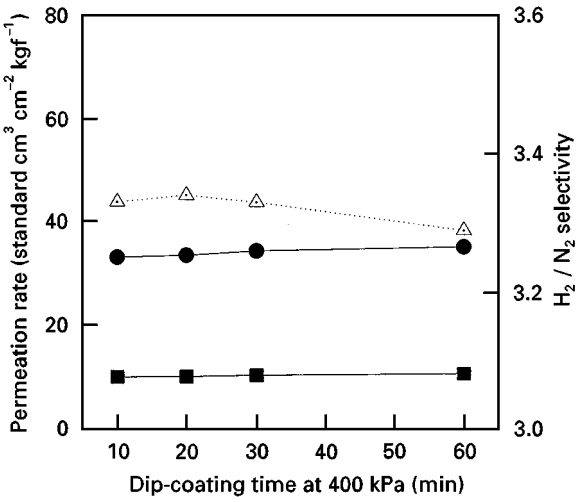

Figure 9 Gas permeation results of alumina membranes prepared by dip-coating at 400 kPa for various dip-coating times. (●) H_2, (■) N_2, (△) H_2/N_2.

transmitted beam, instead of sharp rings or sharp diffraction points which correspond to polycrystalline materials. Therefore, it seems that sols are nearly completely ceramitized, but not fully crystallized by the calcination at 600 °C.

3.2. Membranes obtained by the sol–gel method

When the pressure during dip-coating was 500 kPa and above, the sol solution penetrated through the porous alumina support tube. Because our intention was to fabricate a thin permselective layer on the porous support, all dip-coatings were carried out at 400 kPa throughout this study. In addition, the H_2/N_2 selectivity of a membrane fabricated at 400 kPa was slightly greater than that at 100–300 kPa.

Fig. 9 shows gas permeation results of alumina membranes produced by sol dip-coating at various dipping times. The results are summarized by plotting (a) permeation rates of both gases, and (b) H_2/N_2 selectivity with respect to each variable. The permeation rates of both gases slightly increased as the time was extended. From the viewpoint of selectivity, 20 min dipping seems to be the best ($\sim$3.35) of all. The theoretical H_2/N_2 selectivity for the Knudsen diffusion regime is calculated as 3.74. Therefore, the

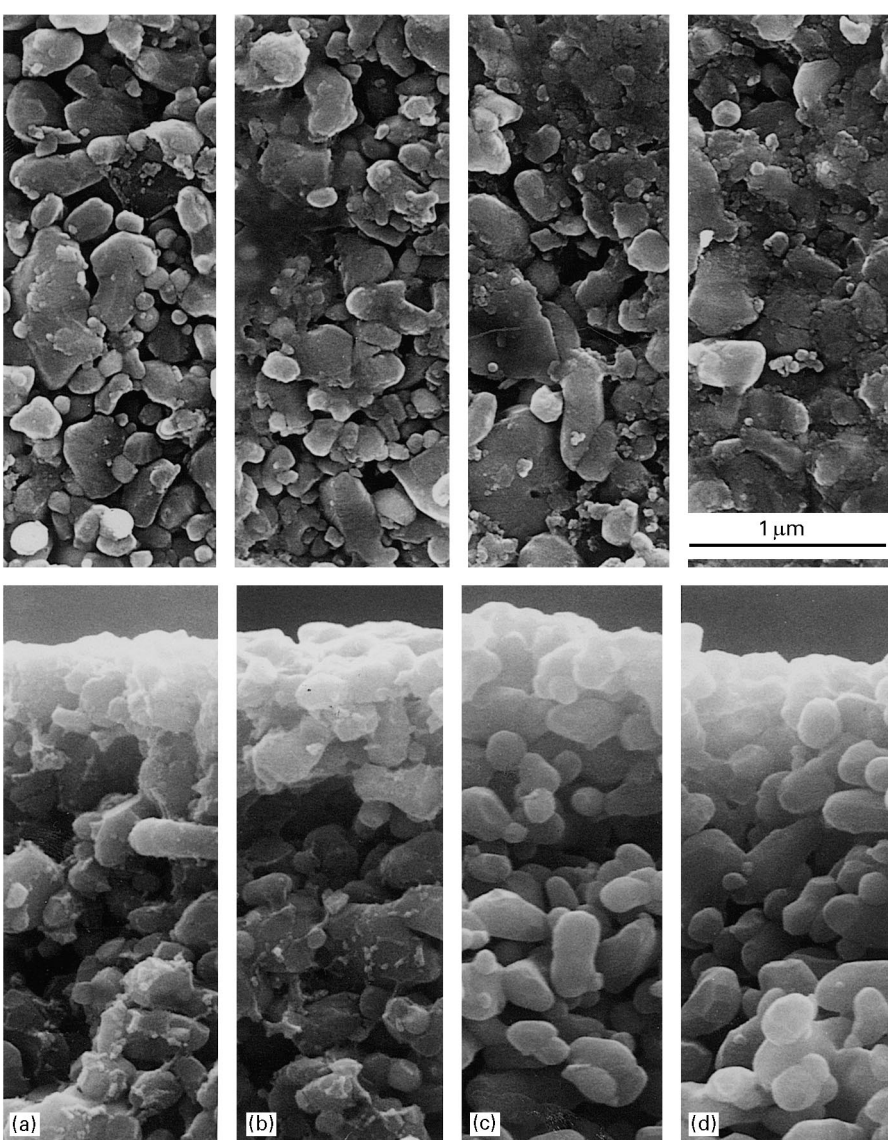

Figure 10 Scanning electron micrographs of surfaces and cross-sections versus dip-coating time: (a) 10 min, (b) 20 min, (c) 30 min, and (d) 60 min.

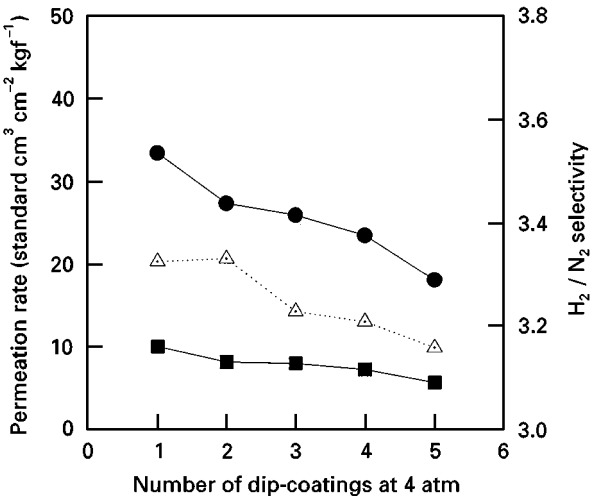

Figure 11 Gas permeation results of alumina membranes prepared by dip-coating at 400 kPa at various numbers of dip-coatings. (●) H_2, (■) N_2, (△) H_2/N_2.

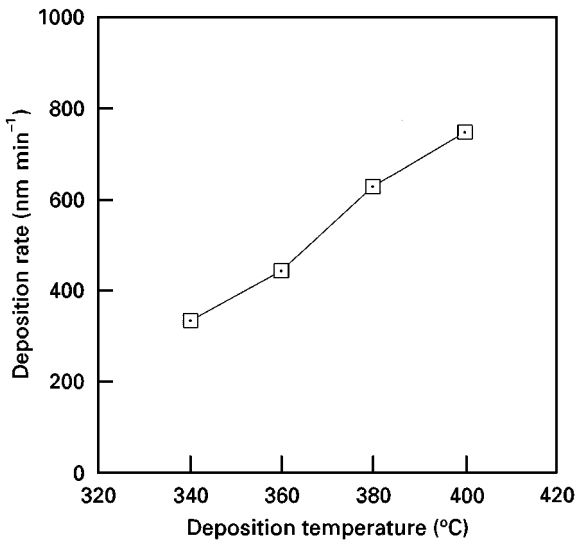

Figure 12 Plot of deposition rate versus deposition temperature.

gas separation by those membranes appears to take place in the Knudsen diffusion regime. When the pore sizes of membranes are smaller than 10 nm, gas separation would occur in a molecular sieve mechanism to give an extremely high H_2/N_2 selectivity.

Fig. 10 shows scanning electron micrographs of surfaces (above) and cross-sections (below) of membranes prepared by dip-coating at various dipping times. Overall, the micrographs look very much alike. By sol dip-coating and calcination at 600 °C, very tiny (smaller than 0.05 μm) new particles were formed on large (0.1–0.5 μm) host particles of porous alumina supports. A shorter dipping time seems to have formed new particles rather deep in the cross-section. After dipping for 10–20 min, the newly-formed particles are evenly distributed throughout the cross-section of the membranes. On the other hand, the formation of new particles was concentrated surface-wide, while host particles at some depth in the cross-section stayed free of tiny particles. The slight difference in the gas permeation performance seems to be attributed to this behaviour.

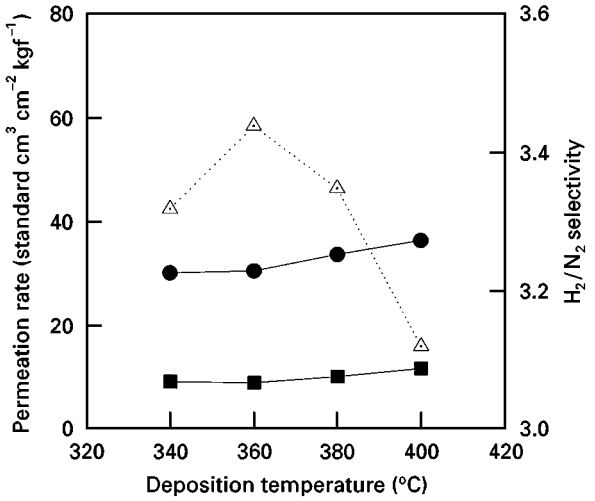

Figure 13 Gas permeation results for membranes prepared by CVD of $Al(Opr^i)_3$ at various deposition temperatures. (●) H_2, (■) N_2, (△) H_2/N_2.

Gas permeation results with respect to the number of dip-coatings are summarized in Fig. 11. Considering both the gas permeation rates and H_2/N_2 selectivity, one dip-coating seems to give the best results.

3.3. Membranes obtained by the CVD method

Fig. 12 illustrates the plot of alumina deposition rate using $Al(OPr^i)_3$ versus deposition temperature. The deposition rates were fairly high, measured as greater than 350 nm min^{-1}. The rate was also linearly proportional to the deposition temperature. The deposition rate using $Al(OPr^i)_2$(etac) versus deposition temperature was not measured easily. Details will be discussed later.

Fig. 13 summarizes gas permeation results for the CVD of $Al(OPr^i)_3$ at various deposition temperatures. As the temperature increased up to 400 °C, the permeation rates of both gases increased with an extremely small slope. Hydrogen permeation rate was just above 30 standard cm^3 cm^{-2} kg^{-1}, slightly greater than that (~35 standard cm^3 cm^{-2} kg^{-1}) of membranes prepared by the sol dip-coating technique. The H_2/N_2 selectivity, on the other hand, reached a maximum (~3.44) at 360 °C.

Fig. 14 shows scanning electron micrographs of surfaces and cross-sections of membranes produced by CVD of $Al(OPr^i)_3$ at 360, 380, and 400 °C. The deposition of alumina took place on the surface of supports. Compared to the porous support, deposited films made a very dense structure with a compact grain structure on their surfaces in the temperature range studied here. The grain size appears to become greater as the deposition temperature increases. Few cracks were found in the film deposited at 400 °C. Those cracks might be partly responsible for the poor gas permeation performance of membranes prepared by CVD of $Al(OPr^i)_3$ at 400 °C.

Fig. 15 summarizes gas permeation results of alumina membranes produced by CVD of $Al(OPr^i)_2$(etac)

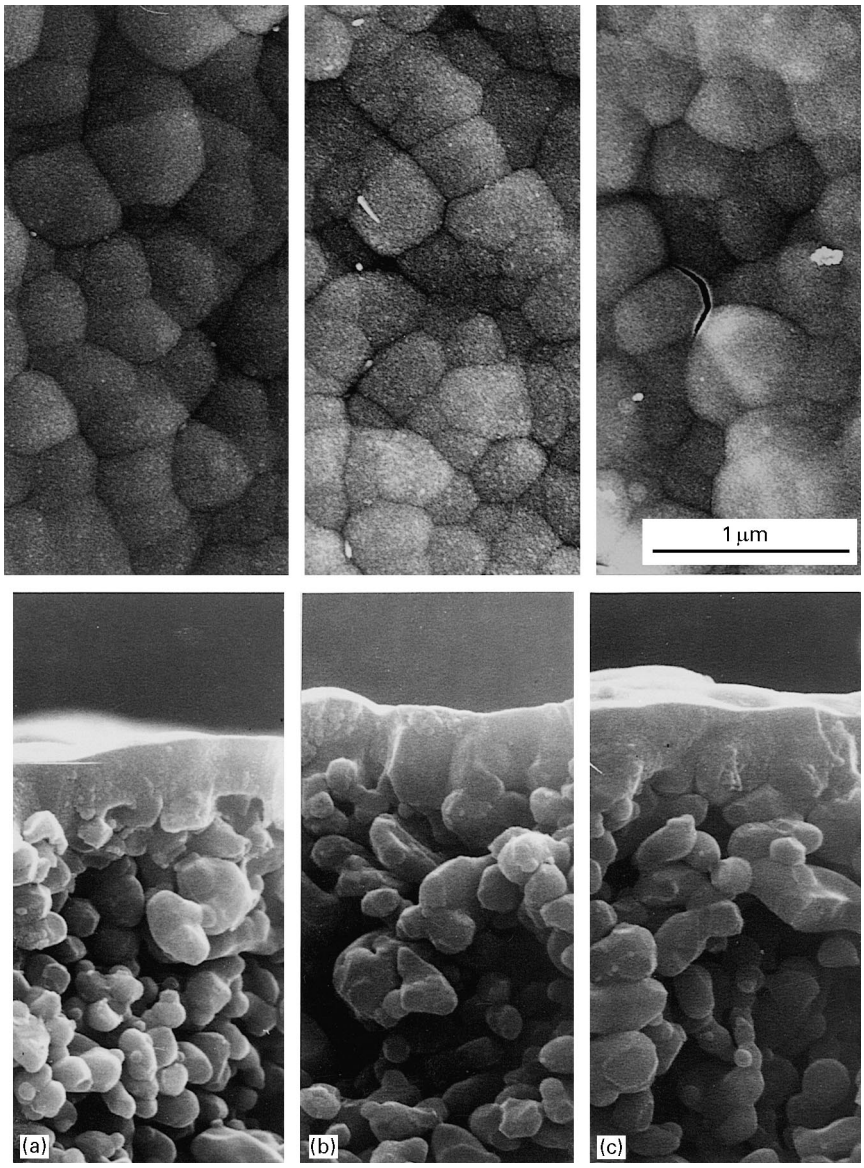

Figure 14 Scanning electron micrographs of surfaces and cross-sections versus deposition temperature: (a) 360 °C, (b) 380 °C, and (c) 400 °C.

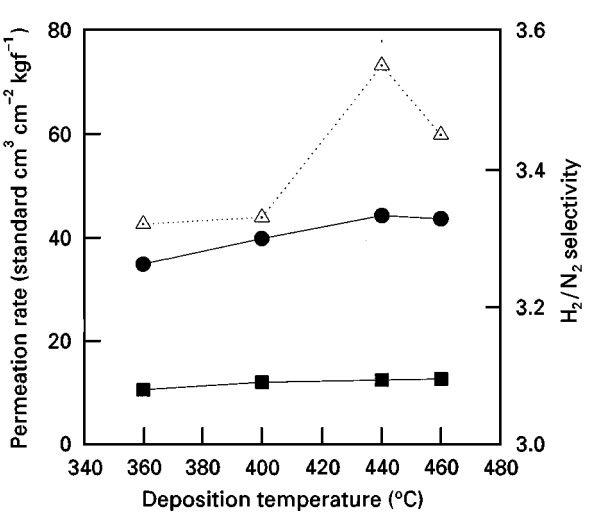

Figure 15 Gas permeation results for membranes prepared by CVD of $Al(OPr^i)_2$ (etac) at various deposition temperatures. (●) H_2, (■) N_2, (△) H_2/N_2.

at various deposition temperatures. Similar to the case of $Al(OPr^i)_3$, permeation rates of both gases slightly increased as the deposition temperature went up. The maximum H_2/N_2 selectivity ($\sim$3.6) was achieved at 440 °C. A comparison of data for $Al(OPr^i)_2$(etac) with those for $Al(OPr^i)_3$ indicated that $Al(OPr^i)_2$(etac) gives a better gas permeation performance either in permeation rate or in H_2/N_2 selectivity than $Al(OPr^i)_3$.

Fig. 16 shows scanning electron micrographs of surfaces (above) and cross-sections (below) of alumina membranes prepared by CVD of $Al(OPr^i)_2$(etac) at 360, 400, and 440 °C. Their micrographs are quite different from those for $Al(OPr^i)_3$. In contrast to those of $Al(OPr^i)_3$, no layer deposited on the porous support was found in cross-sections, irrespective of the deposition temperature. Particles of porous alumina supports were agglomerated by the newly-formed phases to make a semi-continuous morphology. The degree of agglomeration tends to decrease as the deposition temperature was raised. Therefore, there

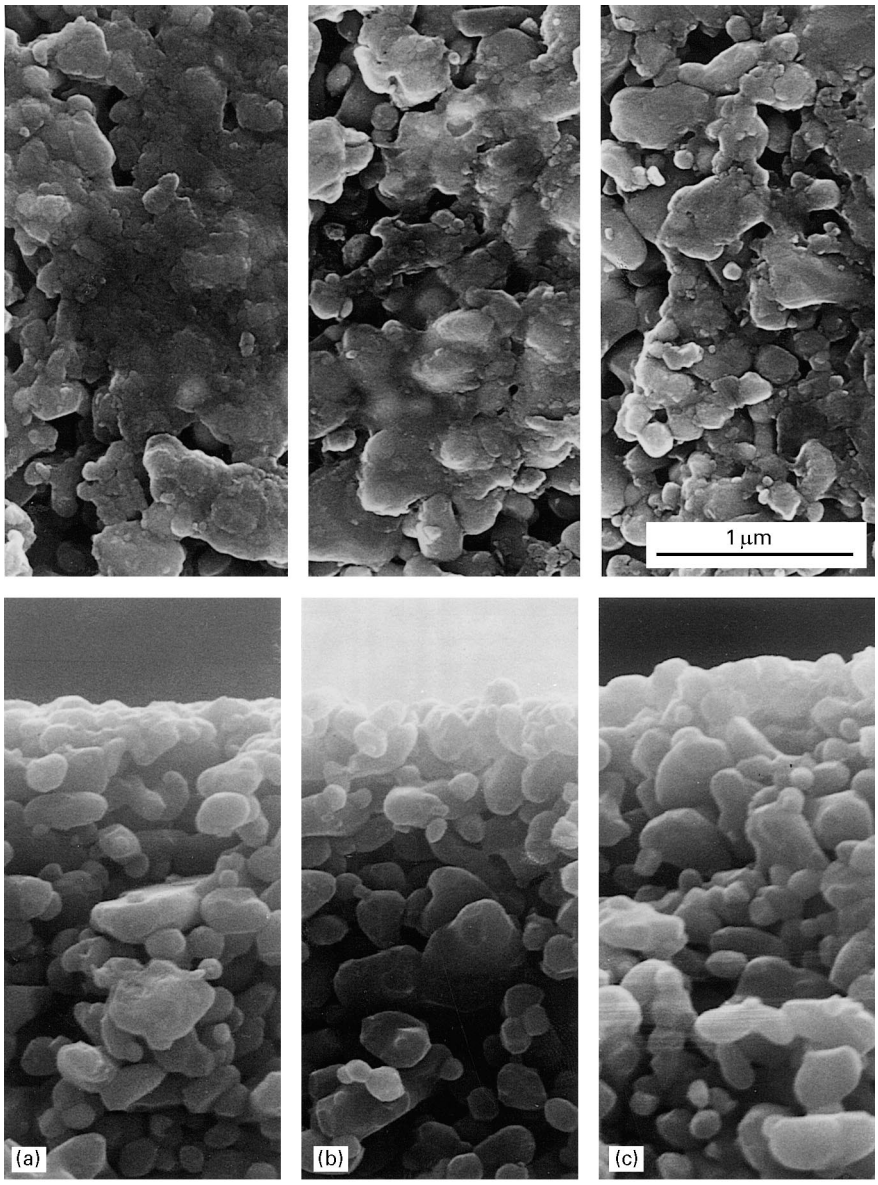

Figure 16 Scanning electron micrographs of surfaces and cross-sections versus deposition temperature: (a) 360 °C, (b) 400 °C, and (c) 440 °C.

should be a substantial difference in the CVD mechanism between those two compounds.

When $Al(OPr^i)_3$ was used as a precursor, the alumina layer seems to be formed mostly by a homogeneous deposition mechanism. Precursor molecules were not able to diffuse into pores of supports before they were thermally decomposed. This behaviour would be partly related to the high feeding rate of precursor molecules to the CVD reactor. It might be also attributed to a rather low activation energy for the thermal decomposition reaction of $Al(OPr^i)_3$. On the other hand, $Al(OPr^i)_3$(etac) molecules have a strong tendency to diffuse into pores of alumina supports where the decomposition reaction mostly takes place. In a manner, the deposition behaviour of CVD using $Al(OPr^i)_2$(etac) is fairly similar to that of the sol dip-coating technique. Experiments to obtain a further detailed explanation are under way.

From the viewpoint of membrane surface morphology, as well as deposition rate, $Al(OPr^i)_3$ looks superior as a CVD precursor to $Al(OPr^i)_2$(etac). Where gas permeation performance is concerned, however, the opposite is true. Another advantage of $Al(OPr^i)_2$(etac), which cannot be overemphasized, is that it is liquid at room temperature. Liquid precursors are heavily favoured in CVD processing, mainly because of the ease and uniformity of source feeding.

3.4. Membranes obtained by combined techniques

Fig. 17 summarizes gas permeation results of membranes fabricated with two techniques combined at various dipping times. $Al(OPr^i)_3$ was used as CVD precursor for this data set. Permeation rates of both gases decreased significantly as dipping time was increased. Nevertheless, when the dipping time was longer than 30 min, the membrane surfaces became rough with many particles on them. The H_2/N_2 selectivity reached a maximum (~ 3.63) at 20 min. A similar trend was observed when $Al(OPr^i)_2$(etac) was used as CVD precursor instead.

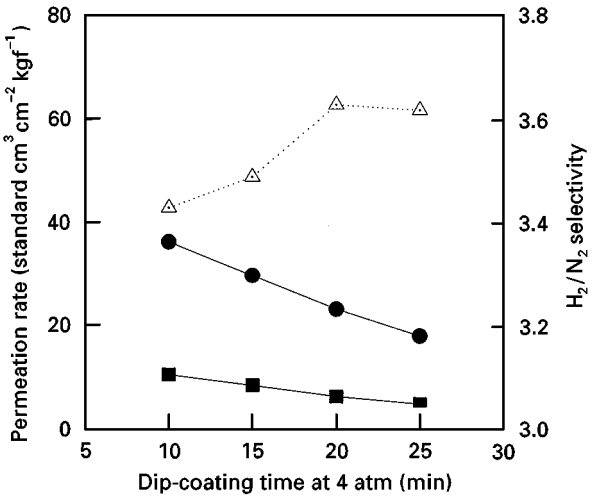

Figure 17 Gas permeation results for membranes prepared by combined techniques at various dip-coating times. (●) H_2, (■) N_2, (△) H_2/N_2.

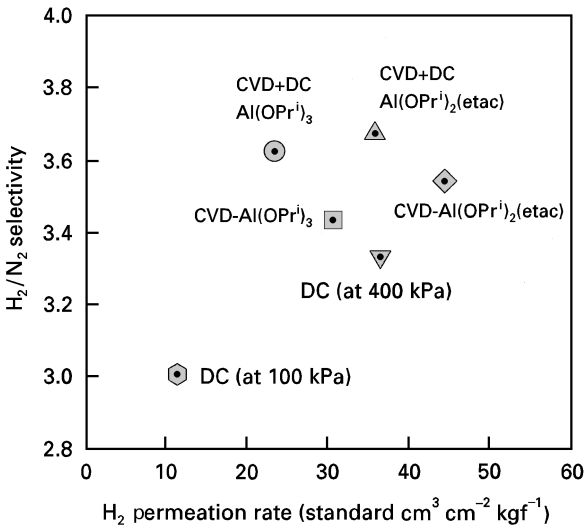

Figure 19 Summarized gas permeation results.

Fig. 18 shows scanning electron micrographs of surfaces and a cross-section of membranes prepared at various dipping times. The membrane fabricated based on 10 min dipping had the least defects on the surface, which would be partly responsible for the highest H_2/N_2 selectivity of all. Scanning electron micrographs of membranes prepared by CVD of Al(OPr^i)$_2$(etac) on dip-coated alumina supports were very similar to those for CVD alone. Hence, their presentation is omitted.

Fig. 19 summarizes gas permeation results of all membranes fabricated in this study. The highest H_2/N_2 selectivity was attained ($\sim$3.7) when the sol dip-coating technique and the CVD technique using Al(OPr^i)$_2$(etac) were combined. On the other hand, the maximum gas permeation rate was achieved when CVD of Al(OPr^i)$_2$(etac) was employed alone. Nevertheless, a theoretical H_2/N_2 selectivity (3.74) for the Knudsen diffusion mechanism was neither reached nor surpassed in either case.

4. Conclusion

A novel alumina precursor was synthesized using a chelating ligand, "etac". The sol formation reaction using Al(OPr^i)$_2$(etac) was greatly reduced for an easy rate control. Polymeric sols derived from Al(OPr^i)$_2$(etac) were found to produce molecules whose size was measured as 2–4 nm. Optimal processing conditions for the sol dip-coating method were determined: a single coating for 20 min at 400 kPa. The CVD deposition behaviours of Al(OPr^i)$_3$ and Al(OPr^i)$_2$(etac), our novel precursor, were substantially different. The former resulted in alumina deposition on the porous support, while the latter caused alumina deposition in the pores of the supports. By combining the sol–gel and the CVD techniques, alumina permselective membranes with improved separation performance were produced.

The highest H_2/N_2 selectivity ($\sim$3.7) was achieved when a sol dip-coating technique was followed by CVD using Al(OPr^i)$_2$(etac). The selectivity was very close to the theoretical one (3.74) predicted by the Knudsen diffusion mechanism. Nevertheless, the selectivity should be substantially improved for a commercial application for a membrane reactor at elevated temperatures.

Acknowledgements

Our research was conducted under a KIST Innovative Research Programme sponsored by the Minister of Science and Technology in Korea.

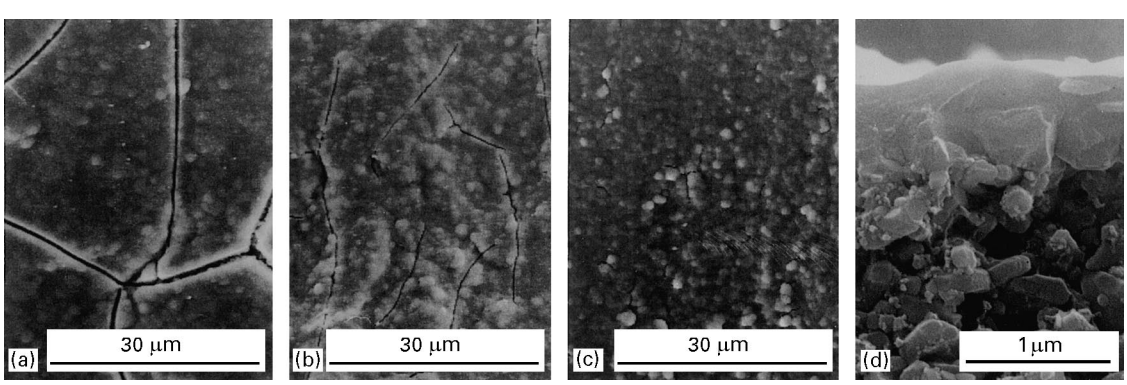

Figure 18 Scanning electron micrographs of surfaces at: (a) 10 min, (b) 15 min, (c) 20 min, and of a cross section at (d) 20 min.

References

1. J. ZAMAN and A. CHAKMA, *J. Memb. Sci.* **92** (1994) 1.
2. K. C. KEITH and M. B. ARTHUR, *Ceram. Memb. Growth Prospects Opportun. C.B.* **70** (1991) 703.
3. R. J. R. UHLHORN, M. H. B. J. HUISIN'T VELD, K. KEIZER and A. J. BURGGRAAF, *J. Mater. Sci.* **27** (1992) 527.
4. A. F. M. LEENAARS and A. J. BURGGRAAF, *J. Coll. Interface Sci.* **105** (1985) 27.
5. R. J. VAN VUREN, B. BONECAMP, R. J. R. UHLHORN, H. J. VERINGA and A. J. BURGGRAAF, *Mater. Sci. Monographs* (*High Tech Ceram.*) **38c** (1987) 2235.
6. A. F. M. LEENAARS and A. J. BURGGRAAF, *J. Memb. Sci.* **24** (1985) 245.
7. *Idem*, *ibid.* **24** (1985) 261.
8. A. F. M. LEENAARS, K. KEIZER, and A. J. BURGGRAAF, *ACS Symp. Ser.* **281** (1985) 57.
9. A. F. M. LEENAARS, K. KEIZER and A. J. BURGGRAAF, in "*Ceram. Adv. Energy Technol.*, edited by H. Krockel, M. Merz and O. Van der Biest (Dordrecht, 1984) pp. 367–386.
10. Y. S. LIN, K. J. de VRIES and A. J. BURGGRAAF, *J. Mater. Sci.* **26** (1991) 715.
11. Y. S. LIN and A. J. BURGGRAAF, *J. Memb. Sci.* **79** (1993) 65.
12. C. J. BRINKER and G. W. SCHERER, in "Sol–Gel Science: The Physics and Chemistry of Sol–Gel Science" (Academic Press, New York, 1990) pp. 235–301.
13. J. H. KIM, H. CHOI, Y. S. CHO and J. C. LIM, *Kor. J. Mater. Res.* **4** (1994) 319.
14. A. ARYRAL, J. PHALIPPOU and J. C. DROGUET, in "Better Ceramics Through Chemistry III", edited by C. J. Brinker, D. E. Clark and D. R. Ulrich (MRS, Pittsburgh, PA, 1988) pp. 239–246.
15. D. R. ULRICH, *Chemtech* April (1988) 242.
16. J. H. KIM, K. S. KIM, S.-T. HWANG, J. I. KIM, J. C. OH and Y. S. CHO, Manufacture of Ceramic Materials by Sol–Gel Method, Annual Report (Seoul, Korea, KIST 1994).

Received 26 February
and accepted 24 September 1997